Eco-Driving Optimization Based on Variable Grid Dynamic Programming and Vehicle Connectivity in a Real-World Scenario

energies

MDPI

Article

Eco-Driving Optimization Based on Variable Grid Dynamic Programming and Vehicle Connectivity in a Real-World Scenario

Luca Pulvirenti, Luigi Tresca, Luciano Rolando * and Federico Millo

Politecnico di Torino, Energy Department, 10129 Turin, Italy; luca.pulvirenti@polito.it (L.P.); luigi.tresca@polito.it (L.T.); federico.millo@polito.it (F.M.)
* Correspondence: luciano.rolando@polito.it

Abstract: In a context in which the connectivity level of last-generation vehicles is constantly on the rise, the combined use of Vehicle-To-Everything (V2X) connectivity and autonomous driving can provide remarkable benefits through the synergistic optimization of the route and the speed trajectory. In this framework, this paper focuses on vehicle ecodriving optimization in a connected environment: the virtual test rig of a premium segment passenger car was used for generating the simulation scenarios and to assess the benefits, in terms of energy and time savings, that the introduction of V2X communication, integrated with cloud computing, can have in a real-world scenario. The Reference Scenario is a predefined Real Driving Emissions (RDE) compliant route, while the simulation scenarios were generated by assuming two different penetration levels of V2X technologies. The associated energy minimization problem was formulated and solved by means of a Variable Grid Dynamic Programming (VGDP), that modifying the variable state search grid on the basis of the V2X information allows to drastically reduce the DP computation burden by more than 95%. The simulations show that introducing a smart infrastructure along with optimizing the vehicle speed in a real-world urban route can potentially reduce the required energy by 54% while shortening the travel time by 38%. Finally, a sensitivity analysis was performed on the biobjective optimization cost function to find a set of Pareto optimal solutions, between energy and travel time minimization.

Keywords: dynamic programming; vehicle-to-everything; real-world scenario; energy minimization; ecodriving; speed optimization

Citation: Pulvirenti, L.; Tresca, L.; Rolando, L.; Millo, F. Eco-Driving Optimization Based on Variable Grid Dynamic Programming and Vehicle Connectivity in a Real-World Scenario. *Energies* **2023**, *16*, 4121. https://doi.org/10.3390/en16104121

Academic Editor: Yi-Hsuan Hung

Received: 3 April 2023
Revised: 5 May 2023
Accepted: 11 May 2023
Published: 16 May 2023

1. Introduction

With climate change threatening the future of our environment and society, implementing immediate and effective strategies to curb Greenhouse Gas (GHG) emissions is the need of the hour. The transportation sector is one of the guiltiest parties, accounting for 35% of the worldwide energy consumption [1]. Since road vehicles, especially passenger cars and road freight transport vehicles, account for 86% of the global share [2], global regulatory targets and customer demand are pushing the automotive industry to develop vehicles with improved fuel economy to reduce GHG emissions [3].

Along with GHG emissions, road congestion is a current problem for transport policy at all levels. According to Joint Research Centre (JRC), the cost of road congestion in Europe is estimated to be over €110 billion a year [4], not to mention the dramatic effects that traffic has on the increased air pollution [5] and environmental noise [6]. This particularly rings true in urban areas, where traffic lights, although being vital for allowing pedestrians and competing flows of traffic to safely cross busy intersections, may lead to increased congestion levels. Besides pollution and congestion, road safety remains a major societal issue [7,8]: only in Europe, more than 19,000 people died on the roads in 2021 and, despite being reduced by 31% compared to 2011 levels, these numbers should continue to fall [9].

In this framework, integrated with the feasible technical solutions aimed at improving the efficiency of current propulsion systems [10], the mass adoption of Connected and

Automated Vehicles (CAVs) may represent an opportunity to tackle the abovementioned issues and could lead, in the next decade, to a major technological revolution in the mobility sector [11], by improving energy utilization efficiency [12], traffic handling [13], and road safety [14].

Creating systems in which information and communication technologies can be easily exchanged, namely Intelligent Transportation Systems (ITS) [15], can be particularly beneficial in urban areas where connected vehicles, featuring Vehicle-to-Vehicle (V2V) and Vehicle-to-Infrastructure (V2I) technologies [16], can have access to the Signal Phase and Timing (SPaT) of traffic lights. This information can be directly transmitted to vehicles through a Dedicated Short Range Communications (DSRC) technology [17] or may become available by the traffic control center through cellular and Wi-Fi networks, namely Cellular Vehicle-to-Everything (C-V2X) [18]. The C-V2X potentiality could be further boosted by a possible coupling with the new 5G mobile network [19] or joint use of DSRC and C-V2X communications [20]. Alternatively, several studies have demonstrated that SPaT information may be inferred via on-board cameras [20] and via crowdsourcing [21].

Traditional approaches focused more on signal control methods to enhance traffic flow at signalized intersections, such as signal timing optimization [22], or actuated signals application in real-world traffic [23] that could allow smoothing traffic oscillations and decreasing vehicle waiting times at intersections. However, with the recent advances in ITS technology that empower the vehicles to share information with the surrounding environment [24], more recent research has been focused on developing ecodriving algorithms, i.e., using the information to plan an optimal path and velocity trajectory so as to improve the efficiency in energy utilization and traffic handling [25].

Some earlier works, like [26], demonstrated how upcoming traffic signal information can be used by a vehicle's adaptive cruise control system to reduce idle time at traffic lights and fuel consumption, or developed algorithms for detecting and predicting the SPaT to enable a Green Light Optimal Speed Advisory (GLOSA) system: i.e., a speed corrector to avoid unnecessary halts at traffic lights [27]. In [28] the performance degradation of the GLOSA system due to queuing effects and actual tracking driver errors is taken into account, while in [29] the uncertainties of SPaT information due to varying patterns of traffic lights are introduced. In the literature, several other applications of ecodriving optimization have been shown: in [30] an algorithm that jointly adjusts vehicle speeds at intersections and signal timings is proposed while in [31] the benefits of incorporating near-term technologies in a predictive management strategy are assessed.

As formalized in [32], eco-driving can be regarded as an optimal control problem where the drive commands are chosen to minimize the energy consumption for a given trip, and, among the set of methods provided by the optimal control theory, some solution techniques that are commonly employed are Model Predictive Control (MPC) and Dynamic Programming (DP). MPC can be implemented as either an optimization problem considering the nonlinearities in the powertrain efficiency characteristics [33] or a computationally less expensive linear optimization problem that only considers the vehicle kinematics [34]. DP [35], as proposed by [29] to optimize the velocity profiles for achieving automated ecodriving, can provide an optimal result even for highly nonlinear problems, such as ecodriving. However, the heavy computation burden of DP has made its use largely limited to asserting an offline performance benchmark, and suitable simplifications are needed to reduce the dimensionality of the optimization problem in real-time applications. For instance, in [36] an algorithm derived from DP that can be real-time implementable is proposed; authors in [37] propose an interesting pruning algorithm aimed at reducing the optimization domain by considering only the portions of the traffic light's green phases that allow driving in compliance with the city speed limits; after defining some points of interest, such as traffic lights, road curvatures, etc.; in [38] a variable step size is introduced that drastically reduces the computation cost; authors in [39] propose a reduction of the search grid by considering the maximum energy recuperation or the maximum battery discharge capacity.

Quite recently, in addition to traditional optimal control theory, Reinforcement Learning (RL) algorithms have also been studied for addressing the ecodriving problem [40]. For instance, authors in [41] propose a hierarchical RL algorithm that decides whether the controlled vehicle should stop or pass at a traffic light and then performs the corresponding longitudinal control accordingly, in [42] ecodriving strategies are developed that are based on RL algorithms that are suitable for cases where little data on the traffic situation are available, and in [43] a hybrid RL-based algorithm is proposed that considers both the longitudinal acceleration/deceleration and the lateral lane changing. Moreover, since the standardization and introduction of vehicular communication is still an ongoing process, and it may take a while to reach a wide penetration rate of CAVs, a lot of research has explored the safety of mixed traffic flow, i.e., CAVs mixed with human-driven vehicles, which, as shown by [44] can be related to platoon size and penetration rate of CAVs.

From the powertrain control point of view, the increasing adoption of connected vehicles can allow for simultaneously optimizing powertrain control and velocity profile. Several studies have explored methods for optimizing the vehicle velocity profile for Battery Electric Vehicles (BEVs) as well as for Internal Combustion Engine Vehicles (ICEVs). In [45], Dynamic Programming (DP) is used to optimize the velocity of a BEV, while in [46], the fuel consumption reduction of a DP-based algorithm is assessed on a heavy-duty ICEV. However, Hybrid Electric Vehicles (HEVs) and plug-in Hybrid Electric Vehicles (pHEVs) can benefit the most from embedding them in an ITS, since the information from the surrounding environment can be used to optimize their control strategies [47,48]. Vehicle-to-Everything (V2X) communication along with cloud computing adoption [49] may enable a change of paradigm of the energy management problem: from an instantaneous optimization to globally minimizing it over the entire driver route [50]. For example, in [51], a hierarchical ecodriving control using MPC under complex driving conditions is designed for connected and automated HEVs where an intelligent driving scenario classifier is devised to identify the driving scenarios.

In summary, many studies optimized vehicle speed by using MPC, RL methods, or strategies derived from DP. All these strategies are inherently suboptimal and only DP can provide the optimal solution, but the heavy computation burden of this strategy has made its use largely limited to asserting an offline performance benchmark. This paper aims to fill these gaps by proposing a preliminary study to assess the potential of a system that could be integrated with cloud computing and interfaced with a real-time implementable energy management strategy. With the recent advances in ITS technology that could empower vehicles to share information with the surrounding environment, it seems feasible that the vehicles can have realistic information about speed limits and Expected Time of Arrival (ETA). In this context, we propose a Variable Grid Dynamic Programming (VGDP) that modifies the variable state search grid on the basis of the V2X information allowing a drastic reduction in the DP computation burden by more than 95% if compared to the standard optimization performed with a fixed grid. These achievements make this algorithm more attractive for real-world applications, and this work can represent a preliminary study that lays the basis for a controller that could realistically consider the DP for online implementation. Figure 1 schematically describes the proposed algorithm: by relying on a cloud computing architecture in which the vehicle communicates its route and destination to a vehicle simulator offsite, the information coming from the surrounding environment, e.g., traffic lights state, speed limits, distance to travel, etc., is used to define a variable state space grid that allows a computationally efficient optimization. The DP can thus define the optimal velocity profile, that the vehicle should follow to optimize the time/energy trade-off. The major contributions of the paper are the followings:

1. Exploiting information coming from the surrounding environment, e.g., traffic lights state, speed limits, distance to travel, etc., to generate a variable state search grid for the DP algorithm: the DP computation burden is reduced by more than 95% if compared to the standard optimization performed with a fixed grid;

2. Assessing the benefits that the introduction of V2V and V2I communication, integrated with cloud computing, can have in a real-world route in terms of energy and time savings. The Reference Scenario is a predefined Real Driving Emissions (RDE) compliant route [52], while the simulation scenarios are generated by assuming two different levels of penetration of V2X technologies. The simulations show that introducing a smart infrastructure along with optimizing the vehicle speed in a real-world urban route can potentially reduce the required energy by 54% while shortening the travel time by 38%;
3. Laying the basis for a cloud-based controller that could realistically consider DP for online implementation: by communicating its route and destination to an offsite vehicle simulator, a connected vehicle could be advised with the optimal velocity profile to follow in order to optimize the energy/time trade-off.

The results of the proposed analysis must be considered as a benchmark since the simulations are carried out for a simplified urban traffic network with vehicles in almost free flow, i.e., without direct constraints related to the preceding or following vehicles, but it can be conceptually extended to the case of multiple vehicles equipped with the proposed algorithm. The rest of the paper is organized as follows. In Section 2, the virtual test rig used for the simulations is introduced along with the description of the simulation scenarios. Then, the ecodriving optimization problem is formulated in Section 3. In Section 4, the results of the optimization algorithm are shown for the two different scenarios. In Section 5, conclusions are summarized and further studies are provided.

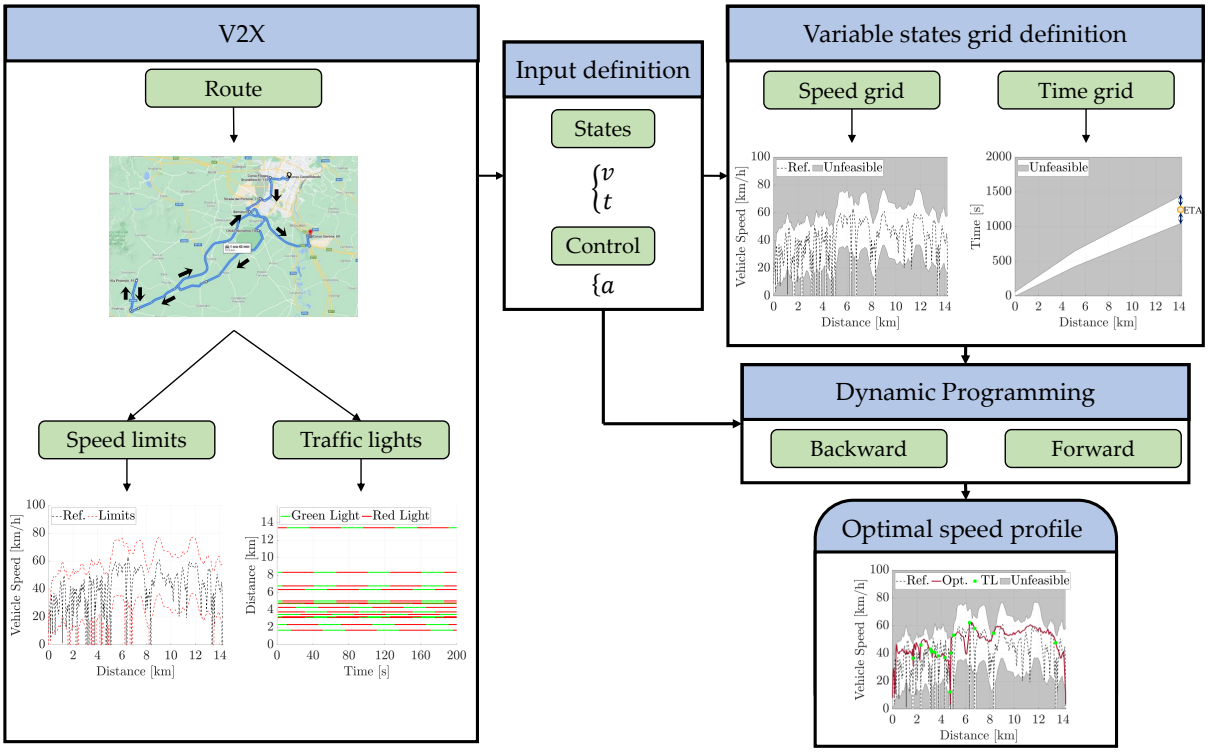

Figure 1. Flowchart of the given algorithm: by relying on a cloud computing architecture in which the vehicle communicates its route and destination to a vehicle simulator offsite, the V2X information is used to define a variable state space grid that allows a computationally efficient optimization. The DP can thus define the optimal velocity profile that the vehicle should follow to optimize the time/energy trade-off.

2. Case Study

2.1. Vehicle Model

The case study is a Mercedes E300de, a state-of-the-art diesel pHEV available in the European market. Figure 2 schematically shows the powertrain layout and Table 1 summarizes the main vehicle and powertrain characteristics. It features a P2 architecture where a Euro 6d-temp 1950 cc diesel engine is integrated into a 90 kW Electric Machine (EM). Both the ICE and the EM are connected, through a torque converter and a 9-speed automatic transmission, to the rear axle. The vehicle was extensively investigated through an experimental campaign, followed by the validation of a virtual test rig against the experimental data, as explained in [53]. In this work, a simplified version of the vehicle model, relying on a backward kinematic model [54] implemented in MATLAB was used. Moreover, since this work presents a powertrain agnostic optimization (i.e., adaptable for each type of vehicle, e.g., ICEV, HEV, pHEV, BEV), the minimization is performed on the energy.

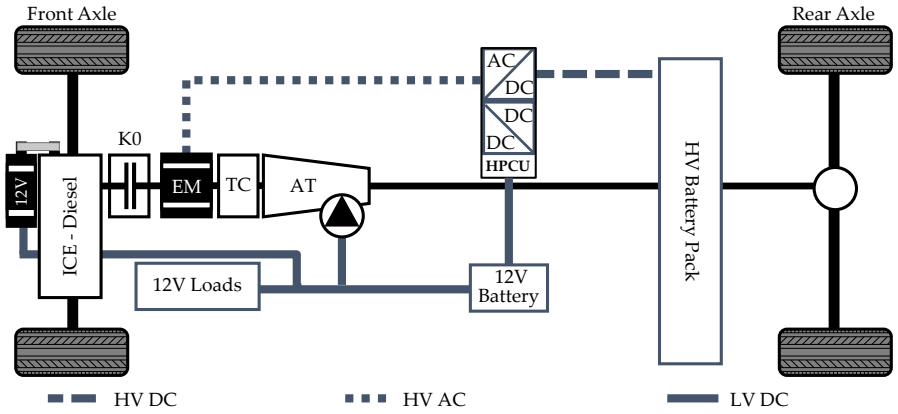

Figure 2. Powertrain layout: a diesel engine is connected through an auxiliary clutch (K0) to an EM. Both the ICE and the EM are connected to the automatic transmission by means of a torque converter.

Table 1. Vehicle and powertrain main specifications.

Vehicle	Curb Weight [kg]	2060
	Power [kW] @ 100 km/h	14.9
Transmission	Type	9-AT w/Torque Converter
ICE	Type	Turbo Diesel
	# of Cylinders	4
	Displacement [cm^3]	1950
	Max Power [kW]	143
	Max Torque [Nm]	400
	Compression Ratio	15.5:1
EM	Type	PM Synchronous Motor
	Max Power [kW]	90
	Max Torque [Nm]	440
	Max Speed [rpm]	6000
Battery	Type	Li-NMC
	Capacity [kWh]	37

2.2. Simulation Scenarios

Energy consumption significantly depends on the route characteristics. In this work, in order to fully collect the variability coming from real-world mission profiles, an RDE-compliant route [52] is chosen as a starting point. The RDE driving cycle is considered as the Reference Scenario, without connectivity. As already described, CAVs technology is largely based on the exchange of different types of data between vehicles (V2V) and with the infrastructure (V2I). Two data types may be differentiated: time-invariant and

time-variant ones. Time-invariant data, i.e., road network architecture, road elevation, road slope, road speed limits, speed bumps, etc., can be accessed via a Geographic Information System (GIS) server [55]. On the other hand, time-variant data, i.e., traffic information, road closings, SPaT, etc., could be available only thanks to V2X communication. In this study, it is assumed that both time-invariant and time-variant data can be available through cellular/Wi-Fi networks to the vehicle and that the optimization problem can be solved in a cloud domain. In this framework, the optimal velocity profile can be sent to the driver in the vehicle domain. Starting from the RDE route, Scenario #1 and Scenario #2 were created.

2.2.1. Reference Scenario

The Reference Scenario represents a typical real-world mission profile. It is an RDE-compliant route [52] conducted on public roads in the surroundings of the Italian city of Turin. The route, shown in Figure 3, lasted approximately 92 min and was 96 km long. The vehicle position was obtained from Portable Emissions Measurement System (PEMS) and combined with a topographic map. In the simulation environment, the speed profile and the vehicle stop of the Reference Scenario are imposed.

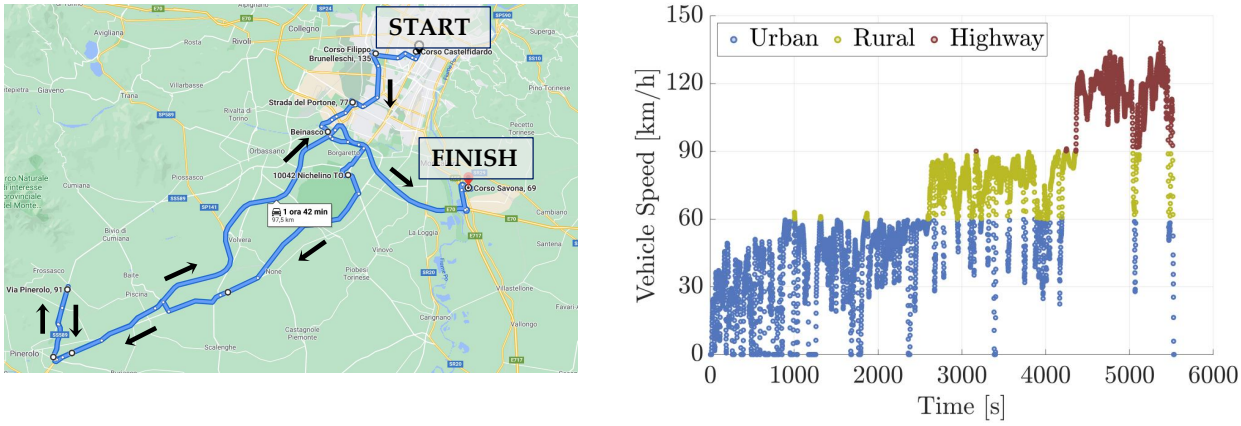

Figure 3. Left: vehicle position obtained from PEMS and combined with a topographic map (Courtesy of Google Maps). The route lasted approximately 92 min and was 96 km long. **Right**: vehicle speed as a function of time divided into urban, rural, and highway sections.

2.2.2. Scenario #1

Scenario #1 was designed to assess the benefits that a global optimization can have on the vehicle speed in a real-world mission profile, still respecting all the full stops imposed by traffic and/or infrastructure. It was generated starting from the Reference Scenario and introducing an intersection regulated by a stop sign every time the vehicle comes to a full stop. The time that the vehicle should wait at each full stop was imposed equal to 23 s: the average time that the vehicle is stationary at the stop signs and red lights in the Reference Scenario. As detailed in Figure 4, a vehicle speed window was created where the optimizer is allowed to range: the window's upper and lower boundaries were thought to merge the effects of speed limits and mild traffic conditions in a realistic scenario. Starting from the speed of the Reference Scenario, the upper and lower boundaries are obtained by applying a moving average over a section of 500 m $\pm$ 20 km/h, respectively. It should be noted that the upper boundary never exceeds 135 km/h, and both the upper and lower ones merge to zero whenever a full stop sign is introduced. As depicted in Figure 5, for Scenario #1, it is assumed that the optimizer can have full access to all the time-invariant data and to traffic information.

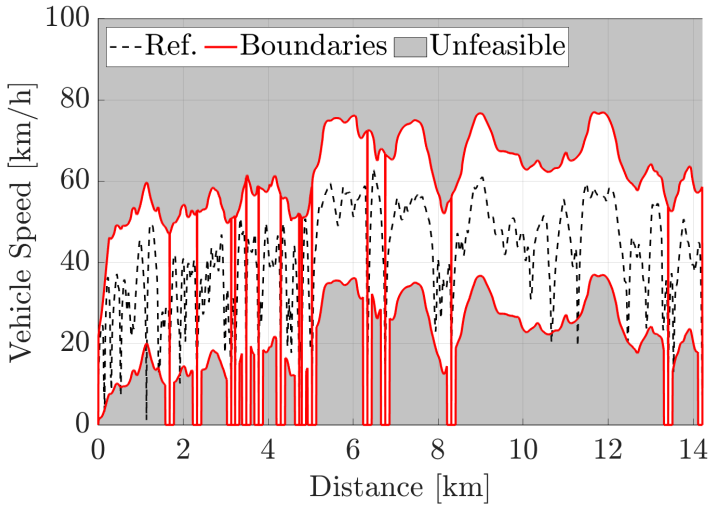

Figure 4. Speed Boundaries: the upper and lower boundaries of the window were thought to merge the effects of speed limits and mild traffic conditions in a realistic scenario.

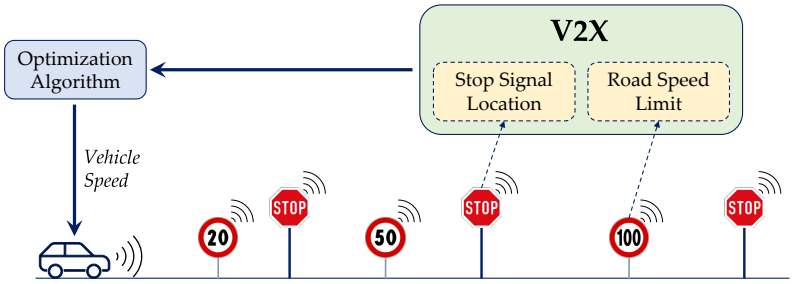

Figure 5. Scenario #1: it was generated starting from the Reference Scenario and assuming an intersection regulated by a stop sign every time the vehicle comes to a full stop.

2.2.3. Scenario #2

Scenario #2 was designed to assess the benefits that the introduction of a smart infrastructure can have on Scenario #1. It was generated starting from Scenario #1 and converting all the stop signs into traffic lights. When designing traffic lights, the quality of the urban realm should be taken into account. According to [56], for urban areas, short cycle lengths of 60–90 s are ideal. Moreover, supposing a minor intersection at each traffic light, a 3:2 ratio is suggested for the amount of green time to improve pedestrian compliance and decrease congestion on surrounding streets. Following these guidelines, in this work, the traffic lights were modeled through square waves with a period and a duty cycle of 1 min and 60%, respectively (the high period corresponds to the green phase). For the sake of simplicity, only red and green phases were considered, while variability was introduced by randomly assigning the initial phase. The speed boundaries coming from Scenario #1 were modified allowing a time-dependent upper boundary in correspondence with the traffic lights, i.e., the upper boundary assumes the moving average value when the traffic light has a green phase. As depicted in Figure 6, it is assumed that SPaT information is deterministic and given; thus, the optimizer can have a priori access to both time-invariant and time-variant data via V2I communication.

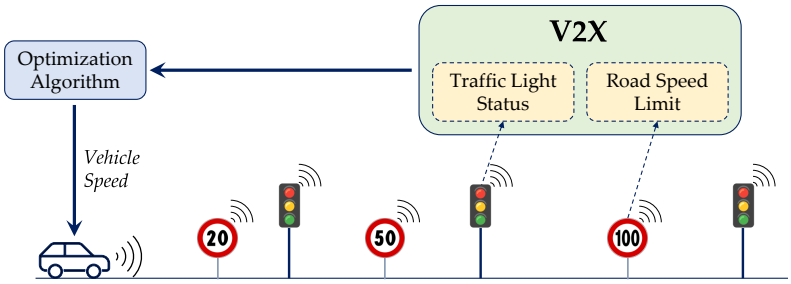

Figure 6. Scenario #2: it was generated starting from Scenario #1 and converting all the stop signs into traffic lights.

3. Ecodriving Optimization

In this section, the algorithm for ecodriving is introduced. It takes advantage of V2X communications and is designed for a simplified urban traffic network with vehicles in free flow, i.e., without direct constraints related to the preceding or following vehicles. V2X information can be used to improve the energy efficiency of a vehicle at two different levels:

- Route optimization: choosing the optimal route;
- Ecodriving: optimize the vehicle speed over the defined route.

This work focuses only on the second stage, i.e., ecodriving. The ecodriving problem can be formalized as an optimal control problem, where the optimizer can access both the vehicle's Global Positioning System (GPS) coordinates (e.g., total trip length, road grade, and speed limits) and V2X information (e.g., SPaT, traffic conditions). Since the position of all the route features varies in a time-based perspective but remains fixed in a distance-based one, it is beneficial to express the model equations in distance-based coordinates: distance (instead of time) becomes the independent variable.

3.1. Optimal Control Problem

In the following, a formulation of the ecodriving problem in distance-based coordinates is proposed:

$$J = \Phi(x(l_f), l_f) + \int_{l_0}^{l_f} L(x(l), u(l), l)\, dl \tag{1}$$

where J is the cost function, $x \in \mathbb{R}^n$ is the vector of the state variable, $u \in \mathbb{R}^m$ is the vector of the control variables, l is the distance variable, $L(x(l), u(l), l)$ is the instantaneous cost function (the variable to be minimized depends on the optimization problem), and $\Phi(x(l_f), l_f)$ is the terminal cost. The cost function is minimized by choosing, in the distance interval $[l_0, l_f]$ the optimal control law $u(l) : [l_0, l_f] \in \mathbb{R}^m$ that leads to the minimization of the cost function. The cost function defined in Equation (1) is subject to the following constraints:

$$\begin{cases} G(x(l), l) \leq 0 \\ x(l) \in X(l) \qquad \forall \quad d \in [l_0, l_f] \\ u(l) \in U(l) \end{cases} \tag{2}$$

where $G(x(l), l) \leq 0$ denotes a generic instantaneous constraint, while $U(l)$ and $X(l)$ are the admissible control and state ranges. Since the main objective of the optimization is to minimize the required energy along with the travel time, the cost function was defined according to the following:

$$J = \int_{l_0}^{l_f} \beta \frac{e_{fd}(x(l), u(l), l)}{E_{fd}} + (1 - \beta) \frac{t(x(l), u(l), l)}{T}\, dl \tag{3}$$

where e_{fd} and t denote, respectively the energy and time demand at the single distance step, while E_{fd} and T denote, respectively, the energy and time demand along the entire cycle.

β is a calibration factor that can be used to trade off between the vehicle energy demand and the traveling time. The constraints for the specific problem concern the physical limitations of the actuators (maximum deliverable power) and of the road infrastructure, e.g., speed limits and traffic lights stop. Additional limits regarding the maximum acceleration and deceleration values were imposed to enhance the driver's comfort in the vehicle. As described in Table 2, the chosen state and control variables for Scenario #1 are vehicle speed and vehicle acceleration, respectively; as for Scenario #2, since the SPaT is time-dependent, the time must be added as a state variable. For speed, acceleration, and time variables a discretization resolution of 1 km/h, 0.01 m/s^2, and 0.5 s were used, respectively, while a discretization resolution of 5 m was used for the independent variable, i.e., distance.

Table 2. State and control variables for Scenario #1 and Scenario #2.

	Scenario #1	**Scenario #2**
State Variables	Speed	Speed, Time
Control Variables	Acceleration	Acceleration

3.2. Dynamic Programming

Dynamic Programming (DP) [35] was used by the Authors to solve the constrained optimal control problem. DP was first introduced by R. Bellman in 1957 [57] and is based on the concept of breaking up sequential decision problems into a finite number of manageable problems wherein the combination of their solutions leads to the global optimal solution of the entire problem. The minimization of the cost function defined in Equation (3) can be expressed in terms of finding the optimal path from the initial location to the final location, by moving backward across a set of discrete states, conventionally called "nodes". Figure 7 sketches an example of how the DP algorithm works referred, for the sake of simplicity, to Scenario #1 (only one state variable, i.e., vehicle speed).

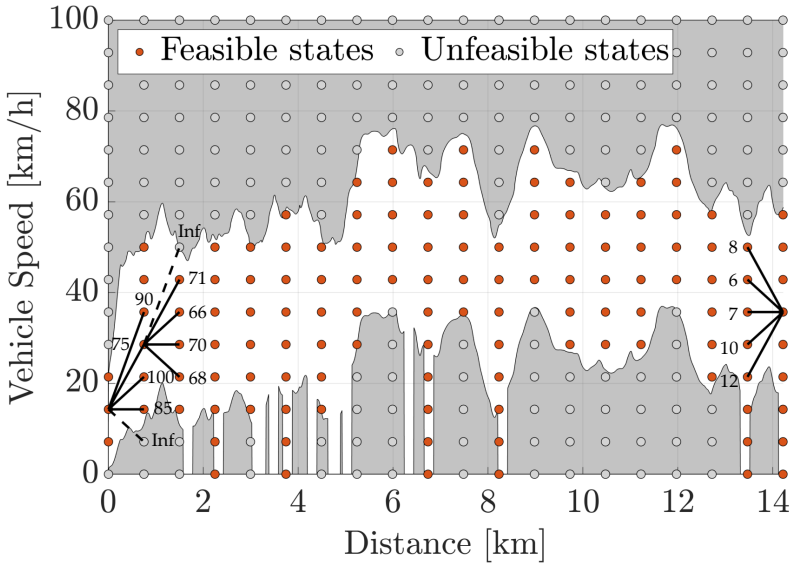

Figure 7. Dynamic programming optimization process shown on Scenario #1: at each distance marker, the DP algorithm finds the set of all feasible nodes (colored ones). Once the costs for all the possible transitions have been computed by proceeding backward in the space domain, the DP algorithm finds the path with minimal cost by moving forward.

At each distance marker in the spatial domain, the DP algorithm first finds the set of all feasible nodes in terms of vehicle speed. Then, the energy demands corresponding to the possible speed transitions are computed, and the constraints expressed in Equation (2) and qualitatively described in Section 3.1 are imposed on the nodes search grid, by assigning a

very large cost to the unfeasible transitions. Once the costs for all the possible vehicle speed transitions have been computed by proceeding backward in the space domain, as Bellman's optimality principle states, it is possible to find the path with minimal cost by moving forward. In this work, the open-source MATLAB code developed at ETH-Zurich [58] was used: it solves discrete-time optimal control problems using Bellman's DP algorithm.

3.3. Variable State Search Grid

As already reported in [59], the Achilles heel of discrete DP is the "curse of dimensionality": in n-dimensional state and m-dimensional control spaces, the number of discrete grid points rises exponentially with the dimensions of n and m [60]. The large computing power needed for the global optimization algorithm has made its use, for the eco-driving problem, largely limited to asserting an offline performance benchmark. This particularly rings true for cases with numerous state variables, like Scenario #2 where time must be added as a state variable increasing the computational burden. However, with the recent advances in ITS technology that could allow vehicles to share information with the surrounding environment, it seems feasible that the vehicles can have realistic information about speed limits and ETA. In this context, a Variable Grid Dynamic Programming (VGDP) can be introduced, which, considering the average traffic information and the estimated time of arrival, reduces the space of the states to only those feasible, and allows for drastically reducing the computation burden of this algorithm. Figure 8 shows the definition of the variable grid in the urban section of Scenario #1. The variable speed grid was defined according to the upper and lower boundaries, supposing that the vehicle can never exceed those limits, while the variable time grid was defined allowing the optimizer to sufficiently vary around a predicted time of arrival.

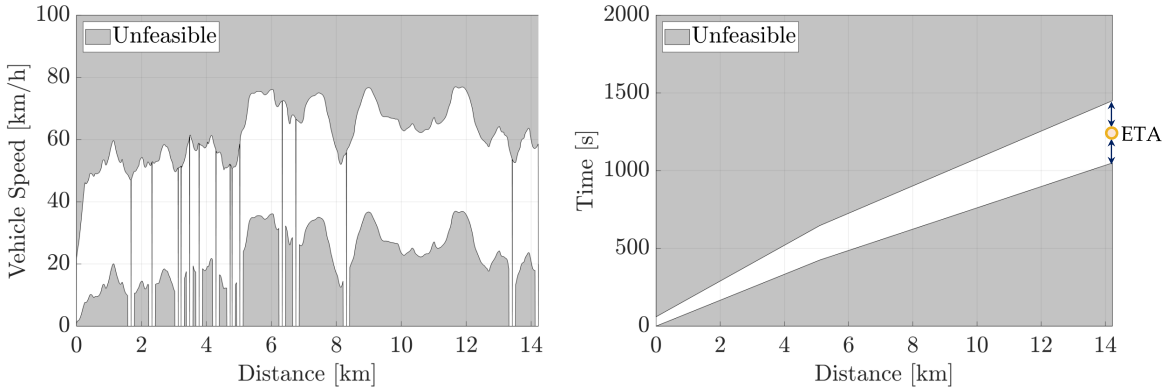

Figure 8. Variable state search grid: the variable speed grid was defined according to the upper and lower boundaries, supposing that the vehicle can never exceed those limits. The variable time grid was defined allowing the optimizer to sufficiently vary around an Estimated Time of Arrival (ETA).

The introduction of the variable state search grid is particularly relevant for Scenario #2 (two control variables). As shown in Figure 9, it allows a reduction in the computational time of more than 95% if compared to the standard optimization performed with a fixed grid, making this technique attractive for a vehicle communicating with a cloud environment. It should be noted that a discretization resolution of 5 m was used for the independent variable, i.e., distance: the higher the discretization resolution (smaller values), the smaller the numerical errors inherently introduced by a discrete DP. Increasing the interval chosen for the distance discretization, despite degrading the accuracy of the solution, can be beneficial for the computational time: a preliminary investigation showed that a $10\times$ increase in the distance step can lead to an $11\times$ reduction in the computational time. The computational times here shown refer to a workstation with the following specifications: Intel(R) Xeon(R) CPU E5-2680 v3 @ 2.50 GHz, 64 GB RAM.

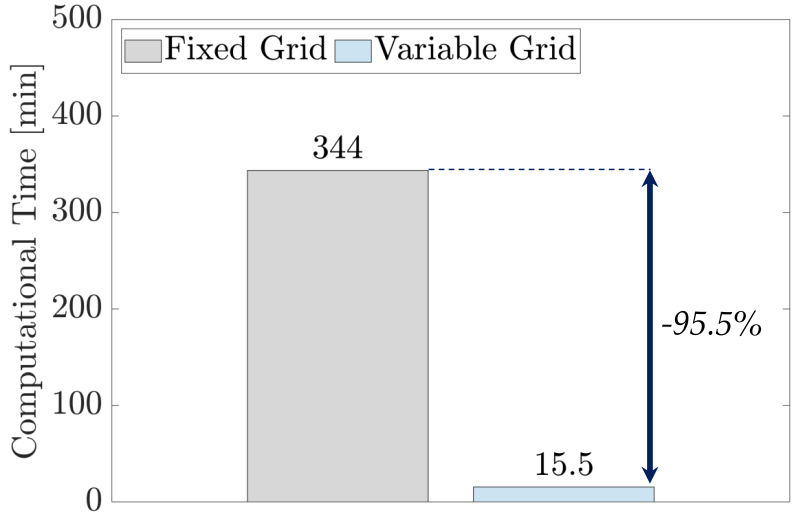

Figure 9. Scenario #2: computational time for the optimal control problem with a fixed state search grid (grey) and a variable state search grid (light blue). The variable grid allows a reduction in the computational time of more than 95%.

4. Results

In this section, the improvements in terms of energy consumption and travel time for Scenario #1 and Scenario #2 are shown. Sections 4.1 and 4.2 show the results for the case with factor $\beta = 0.5$ (see Equation (3)), i.e., the same weight is given to energy and travel time in the cost function. Section 4.3, instead, shows a sensitivity analysis on the weighting factor β. For Scenario #1, the vehicle speed was optimized over the entire selected route in order to assess the performance of the optimization algorithm over different driving patterns, i.e., urban, rural, and motorway. Instead, since most of the traffic lights are present in the urban section, the results for Scenario #2 will be shown only in this case. Thus, the achievable reduction in terms of time and energy reduction will be shown in the entire driving cycle for Scenario #1 and only in the urban profile for Scenario #2.

4.1. Scenario #1

In this section, the optimization algorithm is applied to Scenario #1. This is aimed at assessing the benefits that optimizing the vehicle speed can have in a real-world mission profile, still respecting all the full stops imposed by traffic or infrastructure. Figure 10 shows the optimized vehicle speed for Scenario #1 (blue line) compared to the Reference Scenario (black dotted line). It seems that the optimizer chooses an almost constant speed only in the rural section. In fact, in the urban and highway sections, the vehicle speed tends to follow as much as possible the lower and upper boundaries, respectively. Figure 11 shows a zoom on the urban section. As expected, Scenario #1 presents smoother accelerations and decelerations if compared to the Reference Scenario, although always respecting the full stops imposed by the infrastructure.

Figure 12 shows the achievable reductions in terms of travel time and energy for Scenario #1 considering the entire route (see Figure 10). Nearly 30% of energy reduction can be obtained while decreasing the travel time by almost 10%. These results are achievable while still respecting all the full stops required by the infrastructure analogously to the Reference Scenario. Note also that regenerative braking is not considered in this analysis, so all the energy required for braking is considered lost.

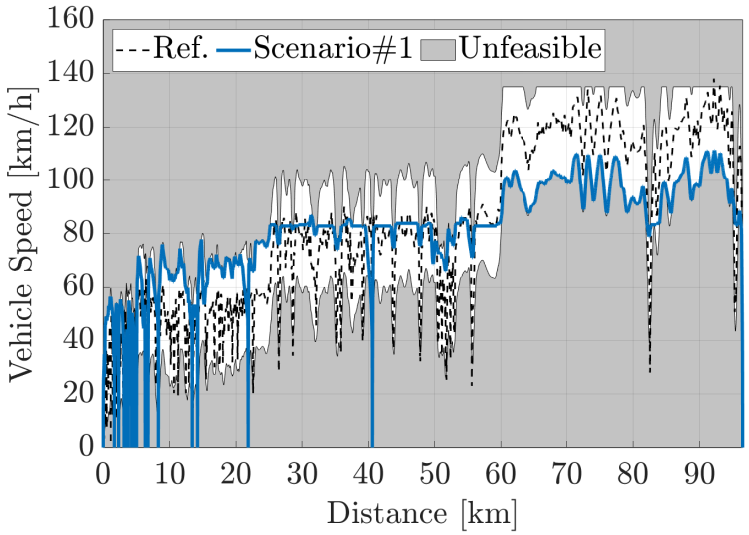

Figure 10. Scenario #1: optimized vehicle speed compared to the Reference Scenario on the RDE-compliant route.

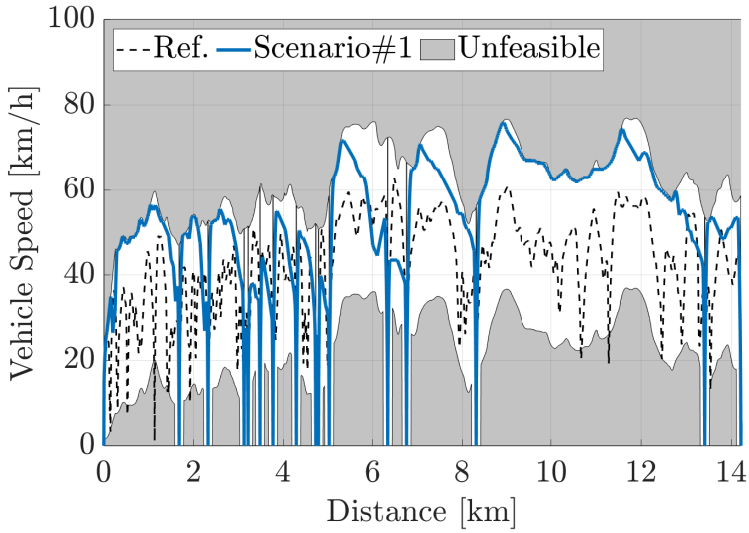

Figure 11. Scenario #1: optimized vehicle speed compared to the Reference Scenario on the urban section of the RDE-compliant route.

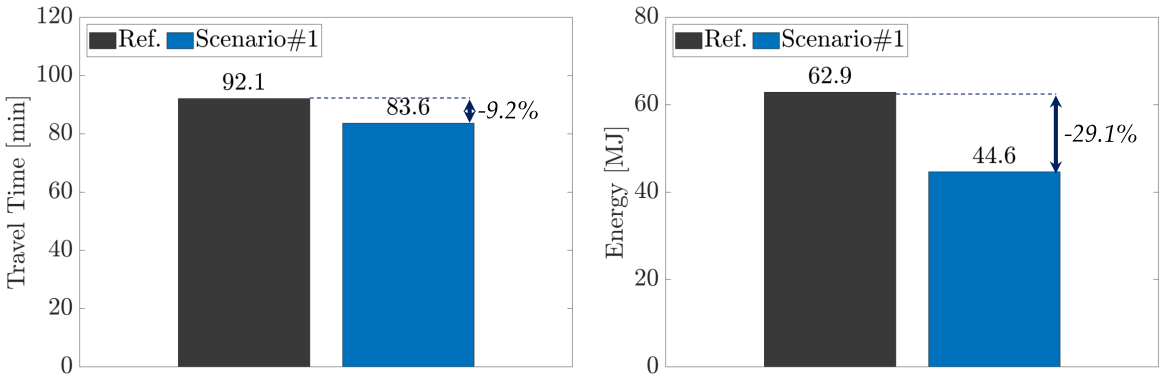

Figure 12. Scenario #1: achievable reductions in terms of travel time and energy on the RDE-compliant route.

4.2. Scenario #2

Since the a priori knowledge of traffic lights SPaT can have major benefits chiefly in an urban environment, the optimization performed by the proposed optimizer will be shown only in these conditions. As already described, Scenario #2 perfectly reproduces Scenario #1 but replaces all the traffic stops with traffic lights. Figure 13 shows the vehicle position as a function of time along with all the traffic light phases. The optimizer chooses the best speed trajectory in order to cross all the intersections at a green light.

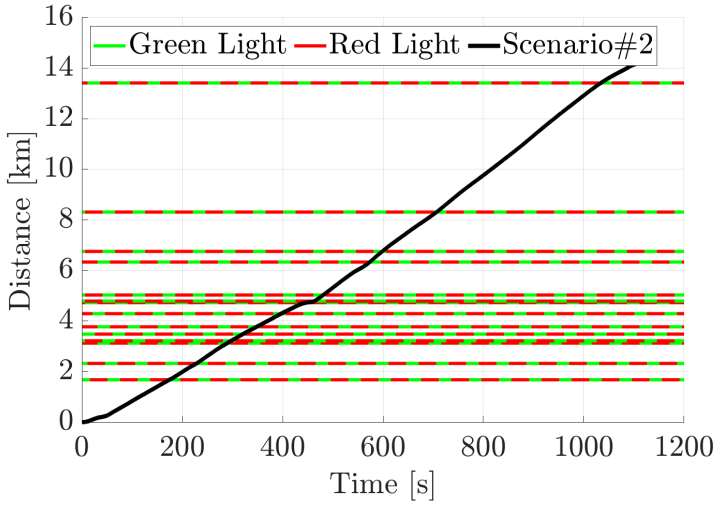

Figure 13. Scenario #2: vehicle position as a function of the time axis along with all the traffic light phases. The optimizer chooses the best speed trajectory in order to cross all the intersections at a green light.

As evident from Figure 14, since the SPaT information is communicated to the optimizer, the vehicle speed is corrected over the entire route to never cross an intersection at a red light. Differently from Scenario #1 (see Figure 11), where the vehicle speed often laid on the upper boundary when the vehicle was not at an intersection, for Scenario #2, an almost constant speed is preferred. The simulations show that a stop sign (or in general a full stop of the vehicle) is detrimental to both the travel time and the energy required. In fact, the deceleration and acceleration phases preceding and following the full stop of a vehicle cause a major reason for energy loss that should be avoided.

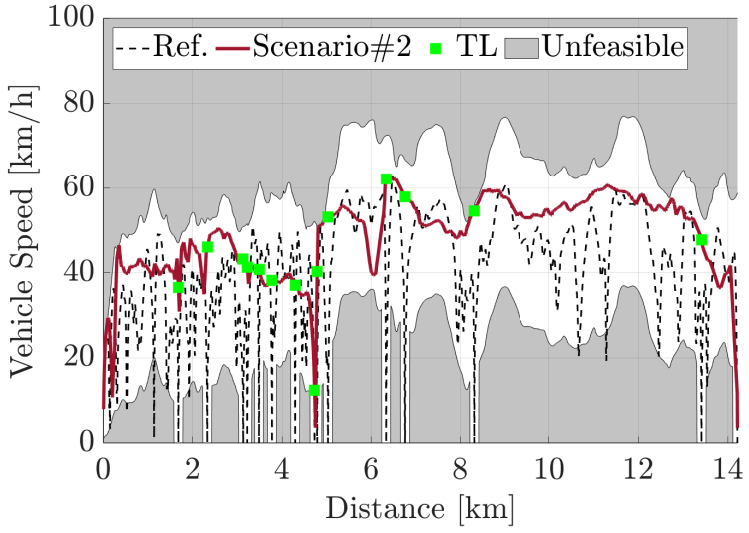

Figure 14. Scenario #2: optimized vehicle speed compared to the Reference Scenario on the urban section of the RDE-compliant route.

A more granular analysis can be done by comparing the characteristic values of the Reference Scenario with the speed profiles optimized by DP. Table 3 displays average and max speed values, min and max acceleration values, and the total time in which the vehicle is stationary during the urban section for all three cases analyzed. The higher vehicle speed values allow reducing the time required for performing the selected route, while the lower acceleration and deceleration values allow for drastically reducing the required energy. The interval of time in which the vehicle is stationary at stops or traffic lights is comparable for Reference Scenario and Scenario #1, while, in Scenario #2, thanks to the exploitation of the SPaT information, the vehicle never crosses an intersection at a red light and thus never stops.

Table 3. Characteristic values of Reference Scenario, Scenario #1, and Scenario #2 on the investigated urban section.

		Reference	**Scenario #1**	**Scenario #2**
Avg. Speed	[km/h]	42	54	49
Max Speed	[km/h]	63	76	62
Max Acc.	[m/s^2]	3.11	1.96	1.96
Min Acc.	[m/s^2]	−3.81	−1.96	−0.98
Standstill Time	[s]	349	398	0

As shown in Figure 15, the introduction of smart infrastructure in the simulated scenario leads to a significant reduction both in terms of travel time and energy. In an urban environment, the energy required by the vehicle can be reduced by half while decreasing the travel time by more than 35%. These findings quantify the maximum achievable reductions in energy and travel time in a framework of connected vehicles able to exploit V2X information in a smart infrastructure.

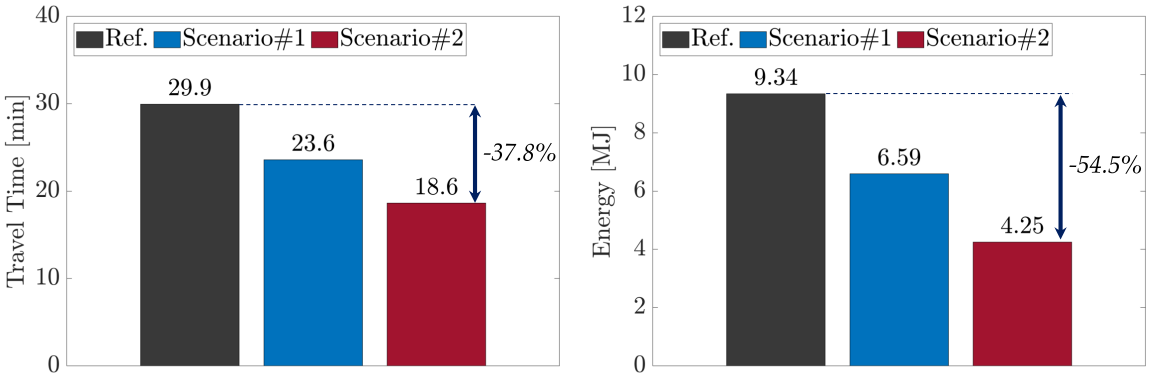

Figure 15. Scenario #2: achievable reductions in terms of travel time and energy on the urban section of the RDE-compliant route.

4.3. Sensitivity Analysis

The sensitivity analysis on the weighting factor was performed to assess the impact that the variation of the relative weights in the cost function can have on the results. In Case 1 ($\beta = 0.2$) travel time is prioritized at the expense of energy. In Case 2 ($\beta = 0.5$) the same weight is given to travel time and energy (results shown in Sections 4.1 and 4.2). In Case 3 ($\beta = 0.8$) energy is prioritized at the expense of travel time. Figure 16 shows the Pareto front between energy and travel time for both Scenarios #1 and #2 when varying the value of the weighting factor, while Tables 4 and 5 provide more granularity by displaying the numerical comparison of the effect of using different values of β.

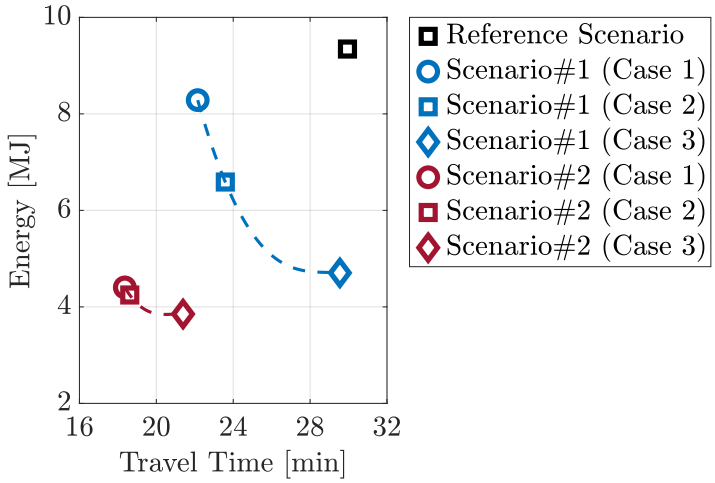

Figure 16. Pareto front between energy and travel time for both Scenario #1 and Scenario #2 when varying the value of the weighting factor β.

Focusing on Scenario #1 (blue marks), for all three cases, the energy consumed to perform the cycle is lower than the Reference Scenario one, mainly due to smoother accelerations and increased cruise traveling time. However, for Case 3 (blue diamond), the excessively conservative driving style, despite decreasing by half the required energy, leads to an increase in travel time if compared to Cases 1 and 2. Focusing on Scenario #2 (red marks), the sensitivity analysis reveals that the introduction of a smart infrastructure (such as connected traffic lights) can further improve the trade-off between required energy and total travel time. Moreover, the sensitivity analysis shows that the variation of the weighting factor in Scenario #2 leads to a much more restrained variation in the energy/time trade-off: prioritizing time does not jeopardize the benefits in terms of energy and vice versa.

Table 4. Scenario #1: numerical comparison of the effect of different β values on the energy consumption and travel time.

		Ref.	Case 1	Case 2	Case 3
Energy	[MJ]	9.3	8.3 −11%	6.6 −29%	4.7 −50%
Travel Time	[min]	30	22 −26%	24 −24%	29 −1%

Table 5. Scenario #2: numerical comparison of the effect of different β values on the energy consumption and travel time.

		Ref.	Case 1	Case 2	Case 3
Energy	[MJ]	9.3	4.4 −53%	4.3 −54%	3.9 −59%
Travel Time	[min]	30	18 −38%	19 −38%	21 −28%

5. Conclusions

Over the next decade, Connected and Autonomous Vehicles (CAV) technologies are expected to become more commonly available on new vehicles. Although their ultimate goal is to improve safety and convenience for customers, they can provide significant information about the planned driver route and the surrounding environment. The knowledge of this information can improve the energy efficiency of a vehicle while reducing, at the same time, travel time. In this framework, this work assessed the benefits that the

introduction of Vehicle-to-Vehicle (V2V) and Vehicle-to-Infrastructure (V2I) communication, integrated with cloud computing, can have in a real-world route in terms of energy and time savings. The Reference Scenario is a predefined Real Driving Emissions (RDE) compliant route, while the simulation scenarios were generated by assuming two different levels of penetration of V2X technologies. The associated energy minimization problem was formulated and solved by means of a global optimization algorithm, i.e., Variable Grid Dynamic Programming (VGDP): relying on information coming from V2X, e.g., traffic lights state, speed limits, distance to travel, etc., a variable state search grid was introduced, which allows reducing the DP computation burden by more than 95%, if compared to the standard optimization performed with a fixed grid. For the route evaluated in this paper, numerical results showed that, in an urban context, introducing a smart infrastructure along with optimizing the vehicle speed can potentially reduce the required energy by 54% while shortening the travel time by 38%. A sensitivity analysis was performed on the biobjective optimization cost function to find a set of Pareto optimal solutions, between energy and travel time minimization. The results of the proposed analysis must be considered as a benchmark since the simulations were carried out for a simplified urban traffic network with vehicles in almost free flow, i.e., without direct constraints related to the preceding or following vehicles, but can be conceptually extended to the case of multiple vehicles equipped with the proposed algorithm. This work represents the first step of a broader activity aimed at developing an integrated framework that can exploit remote cloud computing and V2X information to enhance the fuel economy of HEVs. The cloud-based controller can be used to generate an optimized target speed that can be followed in real-time thanks to a low-level controller, such as an MPC or an AI-based algorithm. It should be noted that a high discretization resolution was used for the independent variable, i.e., distance: increasing the interval chosen for the distance discretization can play a key role in making this technique realistically attractive for an online implementation (a preliminary investigation showed that a $10\times$ increase in the distance step can lead to an $11\times$ reduction in the computational time). Further work will be aimed at testing the entire methodology in a cloud computing interface in order to evaluate its potential to recalculate the optimal velocity profile in response to real-time road traffic information. Moreover, future work will also consider platoon potentialities to address the practicality and safety of more vehicles traveling together.

Author Contributions: Conceptualization, L.P., L.T., L.R. and F.M.; methodology, L.P., L.T. and L.R.; software, L.P. and L.T.; writing—original draft preparation, L.P. and L.T.; writing—review and editing, L.R. and F.M.; supervision, L.R. and F.M.; project administration, F.M. All authors have read and agreed to the published version of the manuscript.

Funding: This research received no external funding.

Data Availability Statement: Data sharing not applicable: data were obtained from the collaboration with companies and are not available for confidentiality reasons.

Conflicts of Interest: The authors declare no conflict of interest.

Abbreviations

The following abbreviations are used in this manuscript:

BEV	Battery Electric Vehicles
CAV	Connected and Automated Vehicle
C-V2X	Cellular Vehicle-to-Everything
DP	Dynamic Programming
DSRC	Dedicated Short Range Communications
EM	Electric Machine
ETA	Expected Time of Arrival
GLOSA	Green Light Optimal Speed Advisory
GHG	Greenhouse Gas

GIS	Geographic Information System
GPS	Global Positioning System
HEV	Hybrid Electric Vehicle
ICE	Internal Combustion Engine
ICEV	Internal Combustion Engine Vehicle
ITS	Intelligent Transportation Systems
JRC	Joint Research Centre
MPC	Model Predictive Control
PEMS	Portable Emissions Measurement System
pHEV	plug-in Hybrid Electric Vehicle
RDE	Real Driving Emissions
RL	Reinforcement Learning
RNN	Recurrent Neural Network
SPaT	Signal Phase and Timing
V2I	Vehicle-to-Infrastructure
V2V	Vehicle-to-Vehicle
V2X	Vehicle-To-Everything
VGDP	Variable Grid Dynamic Programming

References

1. IEA. Largest End-Uses of Energy by Sector in Selected IEA Countries, 2018. Charts—Data & Statistics. Available online: https://www.iea.org/data-and-statistics/charts/largest-end-uses-of-energy-by-sector-in-selected-iea-countries-2018 (accessed on 17 October 2022).
2. IEA. Energy Consumption in Transport in IEA Countries. Available online: https://www.iea.org/data-and-statistics/charts/energy-consumption-in-transport-in-iea-countries-2018 (accessed on 17 October 2022).
3. ICCT. Fit for 55: A Review and Evaluation of the European Commission Proposal for Amending the CO2 Targets for New Cars and Vans. Available online: https://theicct.org/publications/fit-for-55-review-eu-sept21 (accessed on 17 October 2022).
4. Christidis, P.; Rivas, N. *Measuring Road Congestion*; EUR 25550 EN; Publications Office of the European Union: Luxembourg, 2012.
5. Goel, A.; Kumar, P. Characterisation of nanoparticle emissions and exposure at traffic intersections through fast–response mobile and sequential measurements. *Atmos. Environ.* **2015**, *107*, 374–390. [CrossRef]
6. Clark, C.; Paunovic, K. WHO Environmental Noise Guidelines for the European Region: A Systematic Review on Environmental Noise and Cognition. *Int. J. Environ. Res. Public Health* **2018**, *15*, 285. [CrossRef] [PubMed]
7. Čubranić-Dobrodolac, M.; Švadlenka, L.; Čičević, S.; Trifunović, A.; Dobrodolac, M. A bee colony optimization (BCO) and type-2 fuzzy approach to measuring the impact of speed perception on motor vehicle crash involvement. *Soft Comput.* **2022**, *26*, 4463–4486. [CrossRef]
8. Gong, Y.; Lu, P.; Yang, X.T. Impact of COVID-19 on traffic safety from the "Lockdown" to the "New Normal": A case study of Utah. *Accid. Anal. Prev.* **2023**, *184*, 106995. [CrossRef] [PubMed]
9. European Transport Safety Council, Road Deaths in the European Union—Latest Data. Available online: https://etsc.eu/16th-annual-road-safety-performance-index-pin-report/ (accessed on 10 April 2023).
10. Conway, G.; Joshi, A.; Leach, F.; García, A.; Senecal, P.K. A review of current and future powertrain technologies and trends in 2020. *Transp. Eng.* **2021**, *5*, 100080. [CrossRef]
11. Vahidi, A.; Sciarretta, A. Energy saving potentials of connected and automated vehicles. *Transp. Res. Part C Emerg. Technol.* **2018**, *95*, 822–843. [CrossRef]
12. Olin, P.; Aggoune, K.; Tang, L.; Confer, K.; Kirwan, J.; Rajakumar Deshpande, S.; Gupta, S.; Tulpule, P.; Canova, M.; Rizzoni, G. *Reducing Fuel Consumption by Using Information from Connected and Automated Vehicle Modules to Optimize Propulsion System Control*; SAE Technical Paper 2019-01-1213; SAE: Warrendale, PA, USA, 2019; Volume 4, p. 15. [CrossRef]
13. Lu, Q.; Kim, K.D. Autonomous and connected intersection crossing traffic management using discrete-time occupancies trajectory. *Appl. Intell.* **2019**, *49*, 1621–1635. [CrossRef]
14. Papadoulis, A.; Quddus, M.; Imprialou, M. Evaluating the safety impact of connected and autonomous vehicles on motorways. *Accid. Anal. Prev.* **2019**, *124*, 12–22. [CrossRef]
15. European Commission. Directive (EU) 2010/40/EU of the European Parliament and of the Council of 7 July 2010 on the Framework for the Deployment of Intelligent Transport Systems in the Field of Road Transport and for Interfaces with Other Modes of Transport Text with EEA Relevance. Available online: http://data.europa.eu/eli/dir/2010/40/oj (accessed on 10 April 2023).
16. Dey, K.C.; Rayamajhi, A.; Chowdhury, M.; Bhavsar, P.; Martin, J. Vehicle-to-vehicle (V2V) and vehicle-to-infrastructure (V2I) communication in a heterogeneous wireless network—Performance evaluation. *Transp. Res. Part C Emerg. Technol.* **2016**, *68*, 168–184. [CrossRef]

17. Zhu, J.; Roy, S. MAC for dedicated short range communications in intelligent transport system. *IEEE Commun. Mag.* **2003**, *41*, 60–67. [CrossRef]
18. Dimatteo, S.; Hui, P.; Han, B.; Li, V.O. Cellular Traffic Offloading through WiFi Networks. In Proceedings of the 2011 IEEE Eighth International Conference on Mobile Ad-Hoc and Sensor Systems, Valencia, Spain, 17–22 October 2011; pp. 192–201. [CrossRef]
19. Storck, C.R.; Duarte-Figueiredo, F. A Survey of 5G Technology Evolution, Standards, and Infrastructure Associated With Vehicle-to-Everything Communications by Internet of Vehicles. *IEEE Access* **2020**, *8*, 117593–117614. [CrossRef]
20. Ansari, K. Joint use of DSRC and C-V2X for V2X communications in the 5.9 GHz ITS band. *IET Intell. Transp. Syst.* **2020**, *15*, 213–224. [CrossRef]
21. Fayazi, S.A.; Vahidi, A.; Mahler, G.; Winckler, A. Traffic Signal Phase and Timing Estimation from Low-Frequency Transit Bus Data. *IEEE Trans. Intell. Transp. Syst.* **2015**, *16*, 19–28. [CrossRef]
22. Zhang, L.; Yin, Y.; Chen, S. Robust signal timing optimization with environmental concerns. *Transp. Res. Part C Emerg. Technol.* **2013**, *29*, 55–71. [CrossRef]
23. Hao, P.; Wu, G.; Boriboonsomsin, K.; Barth, M.J. Developing a framework of Eco-Approach and Departure application for actuated signal control. In Proceedings of the 2015 IEEE Intelligent Vehicles Symposium (IV), Seoul, Republic of Korea, 28 June–1 July 2015; pp. 796–801. [CrossRef]
24. Zhang, H.; Lu, X. Vehicle communication network in intelligent transportation system based on Internet of Things. *Comput. Commun.* **2020**, *160*, 799–806. [CrossRef]
25. Zhou, Z.; Yang, Z.; Zhang, Y.; Huang, Y.; Chen, H.; Yu, Z. A comprehensive study of speed prediction in transportation system: From vehicle to traffic. *iScience* **2022**, *25*, 103909. [CrossRef]
26. Asadi, B.; Vahidi, A. Predictive Cruise Control: Utilizing Upcoming Traffic Signal Information for Improving Fuel Economy and Reducing Trip Time. *IEEE Trans. Control. Syst. Technol.* **2011**, *19*, 707–714. [CrossRef]
27. Koukoumidis, E.; Peh, L.S.; Martonosi, M.R. SignalGuru: Leveraging Mobile Phones for Collaborative Traffic Signal Schedule Advisory. In Proceedings of the 9th International Conference on Mobile Systems, Applications, and Services, Bethesda, MD, USA, 28 June–1 July 2011; pp. 127–140. [CrossRef]
28. Zhang, Z.; Zou, Y.; Zhang, X.; Zhang, T. Green Light Optimal Speed Advisory System Designed for Electric Vehicles Considering Queuing Effect and Driver's Speed Tracking Error. *IEEE Access* **2020**, *8*, 208796–208808. [CrossRef]
29. Sun, C.; Guanetti, J.; Borrelli, F.; Moura, S.J. Optimal Eco-Driving Control of Connected and Autonomous Vehicles Through Signalized Intersections. *IEEE Internet Things J.* **2020**, *7*, 3759–3773. [CrossRef]
30. Sun, P.; Nam, D.; Jayakrishnan, R.; Jin, W. An eco-driving algorithm based on vehicle to infrastructure (V2I) communications for signalized intersections. *Transp. Res. Part C Emerg. Technol.* **2022**, *144*, 103876. [CrossRef]
31. Baker, D.; Asher, Z.; Bradley, T. *V2V Communication Based Real-World Velocity Predictions for Improved HEV Fuel Economy*; SAE Technical Paper 2018-01-1000; SAE: Warrendale, PA, USA, 2018; Volume 4; p. 11. [CrossRef]
32. Sciarretta, A.; De Nunzio, G.; Ojeda, L.L. Optimal Ecodriving Control: Energy-Efficient Driving of Road Vehicles as an Optimal Control Problem. *IEEE Control Syst. Mag.* **2015**, *35*, 71–90. [CrossRef]
33. Moser, D.; Schmied, R.; Waschl, H.; del Re, L. Flexible Spacing Adaptive Cruise Control Using Stochastic Model Predictive Control. *IEEE Trans. Control Syst. Technol.* **2018**, *26*, 114–127. [CrossRef]
34. Plum, T.; Wegener, M.; Eisenbarth, M.; Ye, Z.; Etzold, K.; Pischinger, S.; Andert, J. A simulation-based case study for powertrain efficiency improvement by automated driving functions. *Proc. Inst. Mech. Eng. Part D J. Automob. Eng.* **2019**, *233*, 1320–1330. [CrossRef]
35. Bertsekas, D. *Dynamic Programming and Optimal Control*; Athena Scientific: Belmont, MA, USA, 1995; Volume 1.
36. Levermore, T.; Sahinkaya, M.N.; Zweiri, Y.; Neaves, B. Real-Time Velocity Optimization to Minimize Energy Use in Passenger Vehicles. *Energies* **2017**, *10*, 30. [CrossRef]
37. De Nunzio, G.; Canudas de Wit, C.; Moulin, P.; Di Domenico, D. Eco-driving in urban traffic networks using traffic signal information. In Proceedings of the 52nd IEEE Conference on Decision and Control, Firenze, Italy, 10–13 December 2013; pp. 892–898. [CrossRef]
38. Ye, Z.; Li, K.; Stapelbroek, M.; Savelsberg, R.; Günther, M.; Pischinger, S. Variable step-size discrete dynamic programming for vehicle speed trajectory optimization. *IEEE Trans. Intell. Transp. Syst.* **2018**, *20*, 476–484. [CrossRef]
39. Back, M.; Terwen, S.; Krebs, V. Predictive powertrain control for hybrid electric vehicles. *IFAC Proc. Vol.* **2004**, *37*, 439–444. [CrossRef]
40. Kiran, B.R.; Sobh, I.; Talpaert, V.; Mannion, P.; Sallab, A.A.A.; Yogamani, S.; Pérez, P. Deep Reinforcement Learning for Autonomous Driving: A Survey. *IEEE Trans. Intell. Transp. Syst.* **2022**, *23*, 4909–4926. [CrossRef]
41. Chen, J.; Wang, Z.; Tomizuka, M. Deep Hierarchical Reinforcement Learning for Autonomous Driving with Distinct Behaviors. In Proceedings of the 2018 IEEE Intelligent Vehicles Symposium (IV), Changshu, China, 26–30 June 2018; pp. 1239–1244. [CrossRef]
42. Wegener, M.; Koch, L.; Eisenbarth, M.; Andert, J. Automated eco-driving in urban scenarios using deep reinforcement learning. *Transp. Res. Part C Emerg. Technol.* **2021**, *126*, 102967. [CrossRef]
43. Guo, Q.; Angah, O.; Liu, Z.; Ban, X.J. Hybrid deep reinforcement learning based eco-driving for low-level connected and automated vehicles along signalized corridors. *Transp. Res. Part C Emerg. Technol.* **2021**, *124*, 102980. [CrossRef]
44. Jiang, Y.; Ren, T.; Ma, Y.; Wu, Y.; Yao, Z. Traffic safety evaluation of mixed traffic flow considering the maximum platoon size of connected automated vehicles. *Phys. A Stat. Mech. Appl.* **2023**, 128452. [CrossRef]

45. Nie, Z.; Farzaneh, H. Real-time dynamic predictive cruise control for enhancing eco-driving of electric vehicles, considering traffic constraints and signal phase and timing (SPaT) information, using artificial-neural-network-based energy consumption model. *Energy* **2022**, *241*, 122888. [CrossRef]
46. Hellström, E.; Ivarsson, M.; äslund, J.; Nielsen, L. Look-ahead control for heavy trucks to minimize trip time and fuel consumption. *IFAC Proc. Vol.* **2007**, *40*, 439–446. [CrossRef]
47. Zhang, F.; Hu, X.; Langari, R.; Cao, D. Energy management strategies of connected HEVs and PHEVs: Recent progress and outlook. *Prog. Energy Combust. Sci.* **2019**, *73*, 235–256. [CrossRef]
48. Pulvirenti, L.; Rolando, L.; Millo, F. Energy management system optimization based on an LSTM deep learning model using vehicle speed prediction. *Transp. Eng.* **2023**, *11*, 100160. [CrossRef]
49. Arthurs, P.; Gillam, L.; Krause, P.; Wang, N.; Halder, K.; Mouzakitis, A. A Taxonomy and Survey of Edge Cloud Computing for Intelligent Transportation Systems and Connected Vehicles. *IEEE Trans. Intell. Transp. Syst.* **2022**, *23*, 6206–6221. [CrossRef]
50. Gupta, S.; Rajakumar Deshpande, S.; Tufano, D.; Canova, M.; Rizzoni, G.; Aggoune, K.; Olin, P.; Kirwan, J. *Estimation of Fuel Economy on Real-World Routes for Next-Generation Connected and Automated Hybrid Powertrains*; SAE Technical Paper 2019-01-1213; SAE: Warrendale, PA, USA, 2020; Volume 4. [CrossRef]
51. Wang, S.; Lin, X. Eco-driving control of connected and automated hybrid vehicles in mixed driving scenarios. *Appl. Energy* **2020**, *271*, 115233. [CrossRef]
52. European Commission. Commission Regulation (EU) 2017/1151 of 1 June 2017 of the European Parliament and of the Council on Type-Approval of Motor Vehicles with Respect to Emissions from Light Passenger and Commercial Vehicles (Euro 5 and Euro 6) and on Access to Vehicle Repair and Maintenance Information, Amending Directive 2007/46/EC of the European Parliament and of the Council, Commission Regulation (EC) No 692/2008 and Commission Regulation (EU) No 1230/2012 and Repealing Commission Regulation (EC) No 692/2008 (Text with EEA Relevance). Available online: https://tinyurl.com/53ecjp7s (accessed on 10 April 2023).
53. Millo, F.; Rolando, L.; Pulvirenti, L.; Di Pierro, G. A Methodology for the Reverse Engineering of the Energy Management Strategy of a Plug-In Hybrid Electric Vehicle for Virtual Test Rig Development. *SAE Int. J. Electrified Veh.* **2021**, *11*, 113–132. [CrossRef]
54. Millo, F.; Rolando, L.; Andreata, M. Numerical Simulation for Vehicle Powertrain Development. In *Numerical Analysis*; Awrejcewicz, J., Ed.; IntechOpen: Rijeka, Croatia, 2011; Chapter 24. [CrossRef]
55. Chang, K.T. *Introduction to Geographic Information Systems*; Mcgraw-Hill: Boston, MA, USA, 2008; Volume 4.
56. Sadik-Khan, J. *Urban Street Design Guide*; NACTO: New York, NY, USA, 2012.
57. Bellman, R. *Dynamic Programming*; Dover Publications: Mineola, NY, USA, 1957.
58. Sundstrom, O.; Guzzella, L. A generic dynamic programming Matlab function. In Proceedings of the 2009 IEEE Control Applications, (CCA) & Intelligent Control, (ISIC), St. Petersburg, Russia, 8–10 July 2009; pp. 1625–1630. [CrossRef]
59. Wahl, H.G.; Bauer, K.L.; Gauterin, F.; Holzäpfel, M. A real-time capable enhanced dynamic programming approach for predictive optimal cruise control in hybrid electric vehicles. In Proceedings of the 16th International IEEE Conference on Intelligent Transportation Systems (ITSC 2013), Hague, The Netherlands, 6–9 October 2013; pp. 1662–1667. [CrossRef]
60. Elbert, P.; Ebbesen, S.; Guzzella, L. Implementation of Dynamic Programming for *n*-Dimensional Optimal Control Problems With Final State Constraints. *IEEE Trans. Control Syst. Technol.* **2013**, *21*, 924–931. [CrossRef]